Annals of Operations Research
https://doi.org/10.1007/s10479-026-07119-8

ORIGINAL RESEARCH

The Path to full bins: integrating effort, social cohesion, and regulation

Francesca Grassetti[1] · **Fabio Lamantia**[2] · **Anastasiia Panchuk**[2,3]

Received: 28 April 2025 / Accepted: 22 February 2026

Abstract
This study explores the recycling dynamics of a society with agents characterized by heterogeneous behavior towards recycling: unconscious agents, who are disengaged and unresponsive to both institutional measures and social incentives, and conscious agents, who actively engage in recycling by weighing the effort involved against intrinsic and societal benefits. A word-of-mouth mechanism regulates the exchange of opinions between agents and possible changes in the attitudes of individuals. The dynamical model takes into account both the share of recyclers and the waste dynamics. Our findings highlight that effective policies must balance effort costs, enforcement mechanisms, and social motivations. While reducing perceived effort costs relative to penalties can theoretically drive total recycling, this approach risks resistance and inequities. Enhancing intrinsic and social rewards through public campaigns and incentives is a more practical strategy to encourage participation. However, intermediate rewards can lead to complex dynamics, emphasizing the need to promote collective participation as a valued norm to ensure stability.

Keywords Circular economy · Heterogeneous agents · Waste dynamics · Word-of-mouth

1 Introduction

Understanding the dynamics behind household recycling behavior is crucial for designing effective and sustainable waste management policies. Despite increasing attention from policymakers and environmental advocates, actual recycling rates often remain below expectations, particularly in contexts where compliance mechanisms are voluntary or weakly enforced. This persistent gap between policy intention and behavioral outcomes calls for

✉ Francesca Grassetti
francesca.grassetti@uniurb.it

Fabio Lamantia
fabio.lamantia@unict.it

Anastasiia Panchuk
anastasiia.panchuk@gmail.com

1 Department of Economics, Society, Politics, University of Urbino, Urbino, Italy

2 Department of Economics and Business, University of Catania, Catania, Italy

3 Institute of Mathematics, National Academy of Sciences of Ukraine, Kiev, Ukraine

Published online: 04 March 2026

a deeper investigation into the mechanisms of individual decision-making and their interactions with institutional and social incentives.

Recycling behavior arises from a multifaceted interaction between individual utility assessments, perceived effort, regulatory enforcement, and social influence. Traditional economic models have primarily focused on cost–benefit trade-offs, exemplified by the seminal contribution of Smith (1972), who introduced a dynamic framework to analyze the substitution between recycling and disposal under conditions of waste accumulation. Following the foundational work of Smith (1972), several extensions have investigated the implications of economic instruments, institutional design, and technological constraints within waste management systems. A substantial body of literature has focused on the role of taxation and the associated costs of waste generation and disposal, showing how pricing mechanisms and Pigovian schemes can enhance efficiency in both recycling and landfilling decisions (Atri & Schellberg, 1995; Eichner & Pethig, 2003; Valente, 2023). Other contributions have emphasized the influence of policymakers in shaping recycling incentives through regulatory frameworks, product design mandates, and waste treatment standards (Di Vita, 2001; Eichner & Pethig, 2001; Hamilton et al., 2013). The tension between recycling efforts and land use has also been explored, particularly through models that incorporate spatial constraints and landfill scarcity, highlighting the trade-offs inherent in sustainable waste policy (Highfill & McAsey, 1997; Huhtala, 1997). Finally, technological aspects have been integrated into dynamic models, accounting for the quality of recycled materials, innovation thresholds, and the systemic instabilities that may arise from imperfect recycling processes or decentralized systems (Lafforgue & Rouge, 2019; Nishimura, 2002).

More recent approaches have emphasized the role of behavioral heterogeneity and the endogenous evolution of preferences. A growing body of research highlights how social norms, habits, and identity formation shape recycling practices: evidence suggests that constructs such as attitude, perceived behavioral control, intention, moral obligation, self-identity, action planning, and past recycling experience are significant predictors of household waste management behavior (Bortoleto et al., 2012; Corsini et al., 2018; Goh et al., 2022; Kipperberg & Larson, 2012; Klöckner & Oppedal, 2011; Pakpour et al., 2014; Thomas & Sharp, 2013; Xu et al., 2017; Yan & Murray, 2023). In parallel, institutional mechanisms such as fines and penalties remain relevant: while perceived behavioral control and attitude are robust predictors of waste sorting intention and behavior, awareness of consequences has been shown to influence personal moral norms more directly than behavioral intention itself (Reijonen et al., 2021; Shi et al., 2021). In line with this, it is increasingly recognized that the link between environmental attitudes and tangible actions is highly complex, and cannot be fully captured by linear or static models (Barr et al., 2001). Addressing this complexity, our work integrates elements from both traditional dynamic modeling and behavioral theories.

While we anchor our analysis in the foundational framework proposed by Smith (1972), we extend it to explicitly account for behavioral feedback: how individuals' decisions are shaped by social influence, perceived effort, financial incentives, and punitive sanctions. From a modeling perspective, our framework draws inspiration from formal models of social learning and behavioral diffusion. Although not initially designed for environmental applications, models such as Dawid (1999) offer rigorous structures for capturing behavior adoption through mechanisms like word-of-mouth and norm-based adaptation. These approaches inform our structure, where recycling decisions evolve through both payoff-based learning and social comparison-dynamics analogous to those found in models of tax compliance and innovation diffusion (see Lamantia and Pezzino (2021)).

Our model contributes to the literature by introducing a two-agent-type framework, distinguishing between *conscious* and *unconscious* individuals. Conscious agents respond to

institutional stimuli and social incentives, and adjust their recycling effort by balancing costs and benefits: they actively participate in recycling and optimize their effort by balancing effort costs with the rewards derived from both intrinsic motivations and societal dynamics. Their utility depends not only on their effort but also on the level of participation in the population, reflecting their sensitivity to social norms. Conscious agents feel increasingly motivated as more people recycle, perceiving their efforts as more effective and meaningful. However, their utility peaks at a certain level of participation and diminishes if societal involvement becomes too high, as they begin to feel their contribution is less necessary. This nuanced behavior makes them responsive to interventions that enhance social norms and collective action. Unconscious agents, on the other hand, remain indifferent to both institutional and social influences, posing unique challenges for policymakers aiming to shift collective behavior: recycling provides no intrinsic or social rewards for them and this makes them impervious to institutional interventions, such as fines, inspections, or taxation, as well as to behavioral incentives like social norms or collective participation. Their rigidity and lack of responsiveness make them a challenging group to influence through traditional policy measures.

We propose a two-dimensional discrete-time model that integrates utility-based optimization, word-of-mouth diffusion, and endogenous waste accumulation. Our formulation enables us to investigate the feedback loop between social dynamics and environmental outcomes, revealing multiple possible fixed points-from universal engagement in recycling to complete disengagement-and assessing their stability. This structure allows us to address fundamental questions in environmental policy: under what conditions do behavioral incentives outperform coercive measures? How does social cohesion promote or hinder sustainable action? And what mechanisms can sustain transitions between distinct behavioral regimes? Additionally, we explore specific societal scenarios, such as those where individuals feel most rewarded when recycling is a rare and distinctive effort, and others where satisfaction grows with widespread collective participation, reflecting differing cultural and social values.

The remainder of this paper is organized as follows. Section 2 presents the theoretical model, detailing the structure of agent interactions and the dynamics of recycling behavior. Section 3 provides a formal analysis of the stability conditions and characterizes the possible long-run fixed points of the system. In Section 4, we provide a global numerical analysis of the dynamical system, highlighting how the main parameters shape its dynamic regimes. Finally, Section 5 offers concluding remarks and policy implications.

2 Model

In this section, we outline the foundational elements of our model, which capture the behavioral and environmental dynamics of recycling. First, we define the utility functions for the two types of agents in the population: conscious and unconscious, detailing how their incentives and decision-making processes differ. Next, we introduce the dynamics of behavioral evolution, modeled through a word-of-mouth framework that describes how social interactions drive changes in the fraction of conscious agents over time. Finally, we present the equation governing the evolution of the waste stock, linking behavioral shifts to environmental outcomes.

2.1 Maximization of agents' utility functions

In a large population of agents, two possible behaviors regarding waste management are considered: either separating waste for recycling or not engaging in recycling. That is, within the population, two distinct types of agents are identified: conscious (c-)agents, who possess knowledge or motivation that encourages them to recycle, and unconscious (u-)agents, who lack such incentives or awareness. We denote by $r \in [0, 1]$ the fraction of agents who participate in recycling activities (c-agents).

The utility framework for the agents considers several components. Let $a > 0$ represent the utility derived from consuming a reference bundle of goods, and $e \geq 0$ denote the effort exerted in recycling waste. The current stock of waste is denoted by $Q > 0$, and all agents are subject to a tax at a rate $\tau \in (0, 1)$, proportional to the existing waste stock. In specifying the taxation mechanism, we deliberately link the tax burden to the stock of waste Q rather than to the inflow A.[1] This modeling choice, although stylized, is consistent with earlier stock-based approaches to environmental taxation (Smith (1972); Eichner and Pethig (2003)).[2] Additionally, unconscious agents may incur a sanction $F > 0$, which occurs with probability $p \in [0, 1]$. Regarding the penalty term F, we deliberately model it as a fixed sanction rather than a function of unrecycled waste. This choice is consistent because unconscious agents are homogeneous: the model's structure implies zero recycling by unconscious agents, so their behavior is uniform across the population. As a result, the fixed penalty F can be interpreted as equivalent to a proportional sanction, since it always applies to the same behavioral outcome (no recycling at all).[3]

The utility of a u-agent, therefore, is defined as follows:

- If not sanctioned, the utility is

$$\pi_{u,n} = a - \frac{\gamma e^2}{2} - \tau Q. \tag{1}$$

- If sanctioned, the utility becomes

$$\pi_{u,s} = a - \frac{\gamma e^2}{2} - F - \tau Q. \tag{2}$$

Thus

$$\pi_u = \begin{cases} \pi_{u,n} \text{ if not sanctioned,} \\ \pi_{u,s} \text{ if sanctioned.} \end{cases} \tag{3}$$

[1] From a modeling perspective, this formulation opens the way for further extensions in which a maximum capacity $Q^{\max}$ is explicitly introduced. Once Q approaches $Q^{\max}$, the system would face sharply increasing costs, reflecting real-world scenarios of landfill saturation. Although a tax based on the inflow A is also meaningful, here we focus on the stock-based approach because it allows us to emphasize precisely these saturation dynamics.

[2] The rationale is that a stock-based formulation captures the cumulative burden of disposal and makes it possible to represent capacity constraints. When the accumulated stock of waste becomes large, landfills approach saturation and municipalities typically incur additional costs, either because waste must be transported to distant facilities or because alternative, more expensive solutions are required. Empirical evidence for the European context, and for Italy in particular, confirms that disposal policies have been strongly affected by capacity constraints and the related cost escalation (Mazzanti and Zoboli (2008)).

[3] While in more general settings with heterogeneous levels of non-recycling, it would be natural to define penalties as a function of the amount of unrecycled waste, in our simplified representation the fixed formulation provides a parsimonious way to capture enforcement without loss of generality. This assumption maintains analytical tractability while still reflecting the idea of deterrence.

Here, the term $-\frac{\gamma e^2}{2}$ captures the disutility of effort in recycling, with $\gamma > 0$ representing the cost parameter associated with the effort. In this framework, recycling effort e is modeled as the disutility of engaging in recycling rather than as a per-unit cost proportional to the quantity of waste recycled. This choice reflects the idea that the main challenge faced by households lies in the adoption and maintenance of recycling behavior, which entails organizational and psychological effort, rather than in the marginal handling of additional waste volumes. Once the practice is adopted, the extra burden of recycling more units is comparatively small.[4]

The utility function for a c-agent is given by

$$\pi_c = a - \frac{\gamma e^2}{2} - k + \alpha e[1 + r(\beta - r)] - \tau Q. \tag{4}$$

This function builds upon the utility components of unconscious agents, with the first two terms representing utility from consumption (a) and the disutility from recycling effort ($-\frac{\gamma e^2}{2}$). The additional term $k > 0$ represents a fixed cost of recycling specific to conscious agents. This cost, absent for u-agents, is assumed to cover the measures taken by c-agents to ensure proper waste sorting, thereby preventing penalties associated with incorrect recycling practices. A key behavioral component of the model is introduced through the term $\alpha e[1 + r(\beta - r)]$, where $\alpha > 0$ is a parameter capturing the behavioral reward of recycling effort as it relates to the fraction r of agents in the population who also engage in recycling. This term reflects two important elements:

- The utility derived from recycling effort reaches a maximum when $r = \beta/2$, where $\beta \in [0, 2]$ modulates the shape of the behavioral reward curve. Beyond this threshold, the utility starts to decline. This reflects a behavioral tendency where individuals perceive diminishing personal necessity to recycle, as the majority of the population already participates. This "free-riding" effect reduces the incentive to contribute further, as individuals assume others are sufficiently addressing the issue.
- The parameter β captures societal norms and expectations regarding recycling participation. For $\beta = 0$, the peak utility occurs when no individuals recycle. This represents societies where individuals derive maximum satisfaction from being part of an exclusive minority contributing to recycling, creating a sense of uniqueness and moral distinction. For $\beta = 2$, the peak utility corresponds to societies where individuals derive greater satisfaction when more members of the community engage in recycling. This reflects a collective mindset where agents feel reinforced by widespread community participation.

This formulation therefore provides a parsimonious way of embedding intrinsic motivation, social norms, and free-riding effects into a unified structure. As noted by Fiorino (2020), pro-environmental behavior is shaped by the interplay of intrinsic motivations, personal values, and identity with external social influences. Our specification reflects this perspective by combining multiple behavioral elements in a single functional form.

The term $-\tau Q$ represents the tax imposed on all agents, proportional to the current stock of waste Q. This component mirrors the corresponding term in the utility function of u-agents, ensuring that both types of agents bear the collective burden of waste management through taxation.

The expected utility of a u-agent is intrinsically linked to the probability of incurring a sanction, reflecting the stochastic nature of behavioral consequences in the model. Specifi-

[4] Although a proportional specification of e could be suitable for different contexts, our fixed-cost formulation provides a parsimonious representation of the behavioral dimension of recycling decisions, consistent with the homogeneous-agent framework considered here.

cally, the expected utility is given by

$$\mathbb{E}[\pi_u(e)] = (1-p)\left(a - \frac{\gamma e^2}{2} - \tau Q\right) + p\left(a - \frac{\gamma e^2}{2} - F - \tau Q\right) = a - \frac{\gamma e^2}{2} - pF - \tau Q, \tag{5}$$

where p represents the probability of being fined. This expression balances two possible outcomes:

- No Sanction: With probability $1 - p$, the u-agent avoids the sanction, deriving utility solely from consumption (a) and incurring costs related to recycling effort ($-\frac{\gamma e^2}{2}$) and the waste tax ($-\tau Q$).
- Sanction: With probability p, the u-agent faces the additional penalty F, reducing their utility.

By analyzing the expected utility framework for u-agents, it becomes evident that these agents always maximize their utility by setting $e = e_u^* = 0$, irrespective of institutional interventions or behavioral influences. This result underscores a critical insight: u-agents represent a subset of the population fundamentally resistant to adopting recycling behaviors. Neither increased enforcement through higher probabilities of fines (p), more severe penalties (F), nor heightened taxation on waste stock (τQ) effectively alters their decision-making. Moreover, the behavioral components present in conscious agents—such as the influence of social norms or collective participation—are absent in u-agents, further solidifying their disengagement. In essence, the u-agents remain impervious to external pressures or communal motivations, opting to minimize effort entirely. This behavioral rigidity highlights a challenge for policymakers: strategies targeting penalties or social incentives are unlikely to shift the behavior of u-agents. Instead, these agents exemplify a population segment that necessitates fundamentally different approaches, such as structural changes in waste management systems or mandatory compliance mechanisms, to address their non-participation in recycling efforts.

The utility function for c-agents differs significantly from that of u-agents due to its deterministic nature. Unlike u-agents, who face uncertainty from potential sanctions, c-agents are exempt from penalties because they engage in proper recycling practices. Their expected utility function is expressed as

$$\mathbb{E}[\pi_c(e)] = \pi_c(e) = a - \frac{\gamma e^2}{2} - k + \alpha e[1 + r(\beta - r)] - \tau Q. \tag{6}$$

We analyze the utility function mathematically to determine the optimal recycling effort that maximizes the utility of c-agents. The first-order condition for maximization is obtained by differentiating π_c with respect to e and setting the derivative to zero:

$$\frac{\partial \pi_c}{\partial e} = -\gamma e + \alpha[r(\beta - r) + 1] = 0.$$

This yields the optimal effort:

$$e_c^* = \frac{\alpha[1 + r(\beta - r)]}{\gamma}. \tag{7}$$

The optimal effort e_c^* is shaped by a balance between the behavioral rewards for recycling and the costs associated with exerting effort. Notice that e_c^* is proportional to the behavioral term $[r(\beta - r) + 1]$, whose effect on utility has been described before. In particular, recall the role of the societal norm parameter β in shifting the peak of the utility of c-agents. The cost of effort parameter γ inversely affects e_c^*. Higher γ values correspond to greater sensitivity to effort costs, reducing the optimal recycling effort.

The willingness of a c-agent to engage in recycling depends on the careful calibration of intrinsic motivations, social norms, and effort costs. This deterministic framework suggests that interventions aimed at increasing r—such as public campaigns to boost recycling participation—can significantly influence the behavior of c-agents. However, overemphasizing communal participation may risk diminishing returns, as agents begin to perceive their efforts as less necessary. Policymakers should therefore consider both the parameters shaping individual behavior and the collective dynamics of recycling to maximize the impact of interventions.

2.2 Evolution of Conscious Agents Fraction Over Time

This section introduces an endogenous mechanism for the changes in the share of conscious agents by embedding it within an evolutionary framework. Consistent with standard approaches in evolutionary dynamics, agents are randomly paired in each period, allowing them to observe and learn from differences in payoffs between behaviors. In a sufficiently large population, this random interaction process supports the assumption that at time t, the fraction r of conscious agents in the population accurately represents the likelihood of any given agent being aware of recycling issues. Let r_t denote the fraction of conscious agents in the population, where the subscript t highlights its time-dependent nature. Behavioral adoption is then governed by updates to this probability, influenced by the expected utilities associated with the two behavioral types: conscious (recycling) and unconscious (not recycling) agents. The evolutionary dynamics are modeled using a word-of-mouth framework, inspired by the methodology presented in Dawid (1999), see also Lamantia and Pezzino (2021). In this setting, social interactions facilitate the spread of behaviors, as agents are more likely to adopt actions that provide greater utility based on observed payoffs.

At each discrete period, two agents are randomly paired and have the opportunity to compare their behaviors and associated utilities. If the paired agents share the same behavior—conscious or unconscious—they will experience identical utilities, leaving no incentive to alter their current choice. In contrast, when a conscious agent interacts with an unconscious agent, the observed utility differential may prompt agents to reconsider their stance. Specifically, a conscious agent might be inclined to adopt the behavior of the unconscious counterpart if the latter's utility is perceived as more advantageous, and vice versa. The likelihood of this behavioral shift is comonotone with the magnitude of the utility difference: the greater the disparity, the stronger the motivation for an agent to switch behaviors.

Word-of-mouth evolutionary dynamics for the evolution of r_t can be expressed by the following difference equation (see for details Appendix A.1):

$$r_{t+1} = r_t \left[1 + (1 - r_t) G\big(y(r_t)\big)\right]. \tag{8}$$

The function $G(\cdot)$ in (8) is a strictly increasing odd function (see Appendix A.1) and

$$y(r_t) := \mathbb{E}[\pi_c(e_c^*)] - \mathbb{E}[\pi_u(e_u^*)] = \frac{\alpha^2[r_t(\beta - r_t) + 1]^2}{\gamma} - k + pF \tag{9}$$

represents the utility difference under optimal effort, where $\mathbb{E}[\pi_c(e)]$ and $\mathbb{E}[\pi_u(e)]$ are given in (6) and (5) respectively with e_c^* in (7) and $e_u^* = 0$.

It is important to emphasize that our specification of the word-of-mouth mechanism should be interpreted as a paradigmatic simplification of reality, in line with the tradition of evolutionary modeling. Evolutionary frameworks commonly adopt stylized dynamics such as replicator rules, logit choice, or word-of-mouth processes, which are mathematically similar

in spirit but differ in the behavioral narrative they convey. Among these alternatives, the word-of-mouth formulation appears particularly suitable for the context of household recycling, where interpersonal communication, imitation, and social comparison play a crucial role in shaping behavioral change.

2.3 Evolution of Waste Over Time

Here, we draw upon the foundational work of Smith (1972): we model the dynamics of waste stock accumulation using the following equation:

$$Q_{t+1} = Q_t(1-\delta) + A - Kr_t e_c^*, \tag{10}$$

where $Q_t \geq 0$ represents the stock of waste at time t, $\delta \in [0, 1]$ denotes the natural decay rate of waste, and A is the exogenous inflow of new waste. The term $r_t e_c^*$ accounts for the effort exerted in recycling by the conscious agents in the population, weighted by the fraction of conscious agents r_t. Notice that while the effort variable e is a behavioral measure of the disutility associated with engaging in recycling, the impact of recycling is represented by the term Ke, where the parameter K serves as a conversion factor. It translates behavioral effort into an effective reduction of the waste stock. Thus, e measures the level of engagement, while K determines the physical efficiency with which this engagement translates into waste reduction. Mathematically, K is a scaling parameter, normalized to 1 in numerical simulations for simplicity.

This dynamic equation highlights the competing forces influencing waste accumulation. On the one hand, natural decay (δ) and recycling efforts ($r_t e_c^*$) act to reduce waste stock. On the other hand, the inflow of new waste (A) contributes to its growth. The interplay of these components determines the temporal evolution of Q, providing the framework for analyzing how recycling behavior and decay mechanisms mitigate waste accumulation over time.

2.4 Modeling the joint dynamics of r_t and Q_t

Building on the dynamics of behavioral evolution (r_t) and waste accumulation (Q_t), we now present the integrated two-dimensional model that describes the joint evolution of these two state variables. Together, these dynamics capture the interplay between the spread of recycling behavior within the population and the resulting changes in waste stock over time.

The dynamics of the fraction of conscious agents are described by equation (8) while the evolution of waste stock is governed by equation (10). Substituting the values of $y(r_t)$ and e_c^* in previous equations, the resulting coupled system is given by the map $\mathcal{S} = (\mathcal{S}_1, \mathcal{S}_2)$ as

$$\begin{cases} r_{t+1} = \mathcal{S}_1(r_t) = r_t\left[1 + (1-r_t)G\left(\frac{\alpha^2[r_t(\beta - r_t)+1]^2}{\gamma} - k + pF\right)\right], \\ Q_{t+1} = \mathcal{S}_2(r_t, Q_t) = Q_t(1-\delta) + A - Kr_t\frac{\alpha[r_t(\beta - r_t)+1]}{\gamma}. \end{cases} \tag{11}$$

The function $G(y)$, which captures the net effect of behavioral switching between agent types based on utility differentials, is derived from an evolutionary word-of-mouth process. The formal derivation and properties of G are presented in Appendix A.1.

The two-dimensional model captures the co-evolution of behavioral awareness and waste stock over time. The first equation governs the spread of recycling behavior within the population, while the second describes the resulting impact on waste accumulation. The interplay between these dynamics highlights the feedback loop wherein increasing awareness reduces waste, while waste levels affect the utilities of agents, further influencing awareness.

3 Existence and stability of fixed points

In this section, we investigate the existence and stability of fixed points in the two-dimensional system. Fixed points represent steady-state solutions where the fraction of conscious agents and the level of waste stock remain constant over time. The analysis begins by identifying the fixed points of the system analytically, solving for the steady-state values of the fraction of conscious agents and waste stock. We then assess the stability of these fixed points by examining the eigenvalues of the system's Jacobian matrix. Stability analysis reveals the parameter ranges and dynamic behaviors under which the system converges to a stable fixed point, oscillates, or exhibits divergent trajectories.

To determine the fixed points of the system, we set $r_{t+1} = r_t = r$ and $Q_{t+1} = Q_t = Q$, reducing the system to solving for the steady-state values of r and Q that satisfy the equations of map $\mathcal{S}$. Through straightforward algebraic manipulations, it can be verified that the fixed points of the system are those summarized in the proposition below.

Proposition 1 *Consider the map $\mathcal{S}$ defined in (11). The boundary fixed points are as follows:*

$$E_n = \left(0, \frac{A}{\delta}\right), \quad E_a = \left(1, \frac{A\gamma - \alpha\beta K}{\delta\gamma}\right), \tag{12}$$

among which the point E_n is always feasible, while E_a is feasible provided that

$$A > \frac{\alpha\beta K}{\gamma}. \tag{13}$$

As for the internal fixed points, there can exist at most two. Namely,

- ***Case 1:*** *If either $k \leq pF$ or $k > pF$ and $\alpha < T$, where*

$$T = \frac{4v}{\beta^2 + 4}, \quad v = \sqrt{(k - pF)\gamma}, \tag{14}$$

  no other fixed points exist.
- ***Case 2:*** *If $k > pF$ and $\alpha > T$, the system admits two more fixed points, $E_1 = (r_1, Q_1)$ and $E_2 = (r_2, Q_2)$ with*

$$r_1 = \frac{1}{2}\left(\beta - \sqrt{\beta^2 + 4\left(1 - \frac{v}{\alpha}\right)}\right), \quad r_2 = \frac{1}{2}\left(\beta + \sqrt{\beta^2 + 4\left(1 - \frac{v}{\alpha}\right)}\right),$$

  $r_1 < r_2$, and

$$Q_i = \frac{A\gamma - Kr_i\alpha\left[r_i(\beta - r_i) + 1\right]}{\gamma\delta}, \quad i = 1, 2.$$

  Moreover, the fixed point E_1 is interior for $\alpha < v$ and $Q_1 > 0$, while E_2 is interior for $\alpha < v/\beta$ and $Q_2 > 0$. The condition $\alpha = T$ corresponds to a fold bifurcation related to the appearance of E_1 and E_2.

Note that the feasibility conditions $Q_1 > 0$ and $Q_2 > 0$ are guaranteed by $A > \max\left\{Kr_1\alpha\left[r_1(\beta - r_1) + 1\right]/\gamma,\ Kr_2\alpha\left[r_2(\beta - r_2) + 1\right]/\gamma\right\}$.

The boundary fixed points correspond to the two extreme cases of recycling behavior within the population. When $r = 0$, no agents recycle, and as a result, the waste stock Q reaches its maximum possible level. Conversely, when $r = 1$, all agents recycle, diminishing the waste stock Q. These boundary cases represent the two polar outcomes in the system, where the collective behavior either entirely rejects or fully embraces recycling.

Previously, we highlighted how the parameter β differentiates societies by shaping the utility derived from recycling. When $\beta = 0$, individuals experience greater utility from recycling when they are part of a small minority, as this exclusivity enhances their perception of impact and moral distinction. In contrast, when $\beta = 2$, the utility of recycling increases with widespread participation, reflecting a collective mindset where individuals derive satisfaction from aligning with communal efforts. This distinction between societies prompts an investigation into how interior fixed points vary across these scenarios in the case where $\alpha > T$. For $\beta = 0$, there always exists a single interior fixed point, E_2, which corresponds to the state where a larger fraction of the population recycles. For $\beta = 2$, however, the only possible interior fixed point, contingent on the value of α, is E_1, where fewer individuals participate in recycling. A final observation concerns the values of v and v/β. Depending on the value of β, v can be either less than or greater than v/β. This relationship underscores how the type of society, as characterized by β, influences the scenario and determines which fixed points can be feasible. The interplay between these parameters highlights the societal impact on the behavioral and environmental outcomes predicted by the model.

With these initial observations, the next step is to assess the stability of the identified fixed points, determining which fixed points are likely to persist under the dynamics of the system. To analyze the stability of the fixed points, we examine the eigenvalues of the Jacobian matrix of the map $\mathcal{S}$. The Jacobian at a generic point (r, Q) is given by:

$$J = \begin{pmatrix} \frac{\partial r_{t+1}}{\partial r} & 0 \\ \frac{\partial Q_{t+1}}{\partial r} & \frac{\partial Q_{t+1}}{\partial Q} \end{pmatrix}.$$

The structure of the Jacobian reveals that it is triangular. Since triangular matrices have their eigenvalues on the diagonal, the eigenvalues of the system are given directly by the diagonal elements:

$$\lambda_1 = 1 + (1-2r)G(y(r)) + r(1-r)G'(y(r))\frac{\partial y}{\partial r}, \quad \lambda_2 = 1 - \delta.$$

This simplifies the stability analysis significantly. Each fixed point is stable if the magnitude of all eigenvalues is strictly less than one, i.e., $|\lambda_1| < 1$ and $|\lambda_2| < 1$. The first eigenvalue, λ_1, depends on the dynamics of r and reflects the behavioral stability, while λ_2, which is constant and independent of r and Q, reflects the stability of the waste dynamics under natural decay.

It is evident that λ_2 always lies within the interval $[0, 1]$, as it depends solely on the natural decay parameter δ. To analyze the values of λ_1, it suffices to recall the key properties of the function G (see Appendix A.1) which enable a detailed characterization of the behavioral dynamics encapsulated in λ_1. Leveraging these insights, we can summarize the stability conditions for the fixed points of the system, which can be formulated in terms of the parameter α and the characteristics of the function G. These results are formalized in the following proposition.

Proposition 2 *Consider the map $\mathcal{S}$ defined in (11). The stability properties of its fixed points are as follows:*

- *The boundary fixed point E_n is stable if $k > pF$ and*

$$\alpha < v \tag{15}$$

with v defined in (14). At $\alpha = v$, the point E_n is non-hyperbolic. Otherwise, E_n is a saddle point with $\lambda_1 > 1$.

- *The boundary fixed point E_a is stable if either $k \leq pF$ or $k > pF$ and*

$$\alpha > \frac{v}{\beta}. \tag{16}$$

  At $\alpha = \frac{v}{\beta}$, the point E_a is non-hyperbolic. Otherwise, E_a is a saddle point with $\lambda_1 > 1$.
- *The interior fixed point E_1 is always a saddle with $\lambda_1 > 1$.*
- *The interior fixed point E_2 is stable if*

$$G'(0) < \frac{\gamma}{\alpha v r_2 (1 - r_2)\sqrt{\Delta}} \tag{17}$$

  with $\Delta = \beta^2 + 4\left(1 - \frac{v}{\alpha}\right)$. With the equality sign in (17) the point E_2 is non-hyperbolic. Otherwise, E_2 is a saddle point with $\lambda_1 < -1$.

Proposition 2 highlights the fixed points that are of particular interest in the system, as only those that can exhibit stability are relevant for long-term dynamics. Both boundary fixed points, E_n and E_a, can be stable under certain parameter conditions, emphasizing their importance in representing extreme states of the population's recycling behavior—either no participation ($r = 0$) or full participation ($r = 1$). However, when considering interior fixed points, only E_2 has the potential to achieve stability, making it a focal point of analysis. The fixed point E_2 is particularly noteworthy because it is the only one capable of undergoing a flip bifurcation. This type of bifurcation is of great significance, as it can lead to the emergence of periodic cycles and, under certain conditions, chaotic dynamics. The possibility of such complex behaviors makes E_2 not just a stable fixed point but also a gateway to richer and more dynamic system evolution. All these aspects will be explored in detail in Sec. 4.

Combining the results of Propositions 1 and 2, we can sketch possible major dynamic regimes of the model.

If $k \leq pF$, regardless of the other parameter values, only boundary fixed points exist, among which E_n is a saddle, while E_a is a stable node. Let us refer to this situation as Regime 1.

If $k > pF$, it is convenient to characterize dynamic scenarios according to the increasing value of α. We note that T always satisfies $T < \min\{v, v/\beta\}$ (which follows directly from (14)). However, the location of v and v/β with respect to each other depends on β.

The case for $\alpha < T$ is similar to the Regime 1 but with the opposite stabilities of the boundary points, that is, E_n is a stable node, while E_a is a saddle. We refer to this situation as Regime 2. Then the fixed points E_1 and E_2 appear at $\alpha = T$ due to a fold bifurcation, generically both being interior, since at the bifurcation $r_1 = r_2 = \beta/2 \in (0, 1)$ for $\beta \in (0, 2)$. And this leads to the occurrence of the interior attractor in the neighborhood of the fixed point E_2. While E_2 is interior, it can undergo a flip bifurcation (provided that equality holds in condition (17)), giving rise to a stable cycle of period 2. A period-doubling cascade may follow, along with further bifurcations that lead to complex dynamics.

As α increases further, the distance between E_1 and E_2 increases and they drift toward the boundary points. At $\alpha = v$ there occurs the transcritical bifurcation of E_n and E_1, so that E_n becomes a saddle, while E_1 becomes a stable node but leaves the feasible region ($r_1 < 0$). At $\alpha = v/\beta$ there occurs the transcritical bifurcation of E_a and E_2, due to which E_a becomes a stable node, while E_2 becomes a saddle and leaves the feasible region ($r_2 > 1$). Finally, consider two extreme cases for β. If $\beta = 0$, at $\alpha = T$ there is $E_1 = E_2 = E_n$. Then the point E_1 is always unfeasible. If $\beta = 2$, at $\alpha = T$ there is $E_1 = E_2 = E_a$, and the point E_2 is always unfeasible.

Figure 1 schematically illustrates the possible dynamic regimes of the map S in the (k, α) parameter plane. The vertical blue line is related to the condition $k = pF$. To the right of this

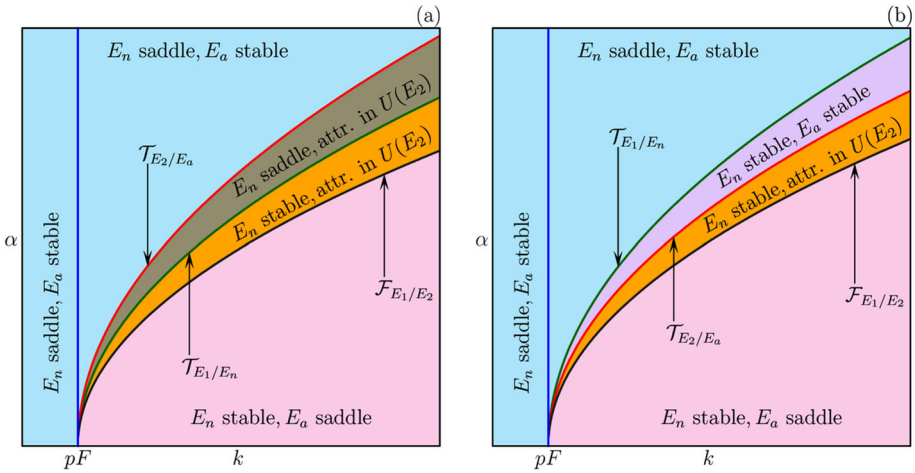

Fig. 1 Schematic representation of the (k, α) parameter plane for (a) $\beta < 1$; (b) $\beta > 1$

line, three other curves correspond to the conditions $\alpha = T$ of the fold bifurcation $\mathcal{F}_{E_1/E_2}$ (black), $\alpha = v$ of the transcritical bifurcation $\mathcal{T}_{E_1/E_n}$ (green), and $\alpha = v/\beta$ of the transcritical bifurcation $\mathcal{T}_{E_2/E_a}$ (red). Note that none of these four conditions depends on the function G; hence, all conclusions drawn below are generic. The function G influences the form of an internal attractor in the neighborhood of the fixed point E_2, as well as the structure of basins of attraction in the case of coexistence.

Dynamics of $\mathcal{S}$ can be summarized as follows.

Regime 1 (with the stable E_a and the saddle E_n) takes place to the left of the blue line related to $k = pF$, as well as to the right of it, above all three curves (the respective region is filled by light-blue).

Regime 2 (with the saddle E_a and the stable E_n) is attained below the fold bifurcation curve, i.e., for $\alpha < T$ (the region highlighted pink).

For the rest, as one can see, there is a slight difference between the cases $\beta < 1$ and $\beta > 1$. In the former case (panel (a)), there is $v < v/\beta$. Then for $T < \alpha < v$, there is:

Regime 3 for a coexistence of the stable E_n and some internal attractor, namely, the stable E_2 or another attractor in its neighborhood $U(E_2)$ (the respective parameter region is highlighted yellow).

Regime 4 for which only the internal attractor remains, is attained for $\beta < 1$ and $v < \alpha < v/\beta$ (gray region).

In the case depicted in panel (b), the relation is the opposite, that is, $v/\beta < v$. Now, for $T < \alpha < v/\beta$, the stable E_n coexists with the internal attractor in the neighborhood $U(E_2)$ (Regime 3), while for $v/\beta < \alpha < v$, there takes place:

Regime 5 with both boundary points, E_a and E_n, being stable (shown by lilac color).

Observe that in Regime 3, the nontrivial[5] internal attractor can disappear due to contact with the boundary of its basin of attraction (as commented further below), in which case

[5] That is, distinct from the fixed point E_2.

Regime 2 is attained. However, when the parameter point is close enough to the respective bifurcation curve, $\mathcal{T}_{E_1/E_n}$ ($\alpha = v$) for $\beta < 1$ or $\mathcal{T}_{E_2/E_a}$ ($\alpha = v/\beta$) for $\beta > 1$, the internal attractor always exists.

As illustrated, Regimes 1, 2, and 4 are related to a single attractor, while in Regimes 3 and 5 coexistence of two different attractors takes place. In both cases, the respective basins of attraction are separated by the stable set of the saddle fixed point E_1. The difference is in the form that this stable set can attain in each case. Recall that the map $\mathcal{S}$ has a triangular shape, namely, its first component $\mathcal{S}_1(r_t)$ does not depend on Q_t (and hence, evolution of the first coordinate r_t can be considered separately). The second component $\mathcal{S}_2(r_t, Q_t)$ is linear with respect to Q_t. And the Jacobian matrix of $\mathcal{S}$ is lower triangular, which implies that the eigenvector for $\lambda_2 = 1 - \delta \in (0, 1)$ is the unit vector $\mathbf{j} = (0, 1)$. Then the initial part of the stable set of E_1 is some vertical line segment l with $r = r_1$. The whole stable set is obtained as a union of preimages of l. If r_1 does not have any other preimages, except itself, with respect to $\mathcal{S}_1$, then all preimages of l belong to the same vertical line defined by $r = r_1$,[6] which exactly composes the target stable set. In this case, the basins of two coexistent attractors are simply connected. For Regime 5, only this scenario is possible, since the part of the function $\mathcal{S}_1$ to the left (right) of r_1 is completely located below (above) the main diagonal, and no additional preimages of r_1 can occur. To sum up, we can state that when both boundary points are stable, their basins of attraction are simply connected and separated by the vertical line $r = r_1$.

In Regime 3, function $\mathcal{S}_1$ has two intersections with the main diagonal in the interval $(0, 1)$. Hence, when the eigenvalue λ_1 of the fixed point E_2 becomes negative, at least one point of a local maximum (in the interval (r_1, r_2)) and one point of a local minimum (in the interval $(r_2, 1)$) of $\mathcal{S}_1$ inevitably appear. If the value of $\mathcal{S}_1$ at some local minimum point $r_m \in (r_2, 1)$ becomes $\mathcal{S}_1(r_m) = r_1$, there occur additional preimages of r_1 located in the interval $(r_2, 1)$. Since the slope of $\mathcal{S}_1$ in the neighborhood of $r = 1$ is greater than one (for E_a its eigenvalue $\lambda_1 > 1$), there is an infinite number of such preimages of r_1 and they converge to $r = 1$ from the left. As a consequence, for the parameter values such that $\mathcal{S}_1(r_m) \le r_1$, the stable set of E_1 consists of infinitely many vertical lines, each corresponding to a particular preimage of r_1. This stable set structure implies one of the following transformations of the phase space.

(1) There is still a coexistence of two attractors, the internal attractor and the stable E_n, each having a disconnected basin with an infinite number of connected elements, and the boundaries of these basins are given by the stable set of E_2 (cf. Example 2 in Sec. 4, illustrated in Figure 4).

(2) While $\mathcal{S}_1(r_m) < r_1$, the internal attractor can expand and at some point undergo a boundary crisis (the attractor collides with the boundary of its basin of attraction and disappears). Then only the stable fixed point E_n remains, implying Regime 2. This dynamic regime holds until the shape of $\mathcal{S}_1$ changes so that there is again $\mathcal{S}_1(r_m) \ge r_1$ and the internal attractor reappears. The latter inevitably occurs when the parameter values approach the bifurcation curve $\mathcal{T}_{E_2/E_a}$ or $\mathcal{T}_{E_1/E_n}$.

[6] Indeed, let us consider a point $(\bar{r}, \bar{Q})$ and find its preimages $(\hat{r}, \hat{Q})$, such that $\mathcal{S}(\hat{r}, \hat{Q}) = (\bar{r}, \bar{Q})$, or, rewritten componentwise, $\mathcal{S}_1(\hat{r}) = \bar{r}$ and $\mathcal{S}_2(\hat{r}, \hat{Q}) = \bar{Q}$. The first equation is independent of the second one and, solved for $\hat{r}$, provides, say, s solutions $\{\hat{r}_1, \ldots, \hat{r}_s\}$. Substituting the latter to the second equation, we obtain exactly one solution $\hat{Q}_i$ for each $\hat{r}_i$ (since $\mathcal{S}_2$ is linear for $\hat{Q}$). In such a way, the number of different preimages is controlled by $\mathcal{S}_1$ only.

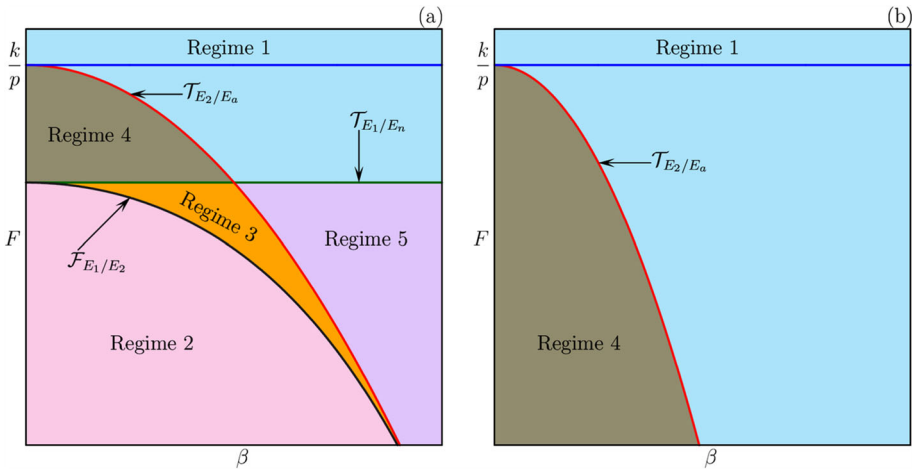

Fig. 2 Schematic representation of the (β, F) parameter plane for (a) $\alpha < \sqrt{k\gamma}$; (b) $\alpha > \sqrt{k\gamma}$

Note that the analytical derivation of the condition related to $\mathcal{S}_1(r_m) = r_1$ is impossible in the general case, since it depends on the form of G. Moreover, it could be impossible even when G is known (for instance, this is the case with the form of G used in Sec. 4).

To finalize an overview of possible dynamic regimes of the map S, in Figure 2, we plot schematically (β, F) parameter plane for two different values of α. The colors of lines and regions have the same meaning as in Figure 1. If $\alpha < \sqrt{k\gamma}$ (panel (a)), all five dynamic regimes, described above, are revealed. Panel (b) shows the situation for $\alpha > \sqrt{k\gamma}$, when the condition $\alpha = v$ (related to the transcritical bifurcation $\mathcal{T}_{E_1/E_n}$) holds for negative F. In this case, there is always a single attractor, a stable E_a (Regime 1) or an internal attractor (Regime 4).

4 Numerical analysis and socio-economic implications

In this section, we explore how policy interventions that influence the key parameters α, p, and F can shape the dynamics of the system. These parameters represent the behavioral rewards for recycling (α), the probability of sanctions (p), and the severity of penalties (F), respectively.[7] By modifying these factors, policymakers can directly impact the stability and existence of fixed points, alter the behavioral composition of the population, and potentially drive the system toward more sustainable waste management outcomes. As discussed in the previous section, two additional key factors shaping the dynamics are the recycling cost (k) and the inherent social norms governing recycling participation (β). The analysis will focus on understanding the sensitivity of the system to these parameters and the implications for designing effective interventions.

The initial analysis concentrates on the parameters p and F, whose product constitutes a critical determinant of the system's dynamics and shapes the behavioral outcomes within the population. As it has already been mentioned, if the product $pF > k$, the system admits only boundary fixed points (Regime 1). In this case, the only stable fixed point is $E_a = (1, Q_a)$,

[7] In fact, the parameters p and F appear in the expression for map $\mathcal{S}$ only as the product pF, which means that any change in p can be compensated by the appropriate change in F and vice versa.

where the entire population adopts recycling behavior. This result arises because the cost of failing to recycle, as represented by the expected penalty pF, exceeds the fixed cost k incurred by conscious agents for proper waste sorting. Consequently, unconscious agents are driven to transition toward recycling behavior, eliminating the possibility of mixed or interior fixed points. The stability of E_a under these conditions underscores the effectiveness of strong enforcement mechanisms in achieving universal recycling participation. From a policy perspective, this finding suggests that increasing either p or F could be a powerful tool to promote recycling behavior across the entire population. By raising the perceived or actual consequences of neglecting recycling, policymakers can shift the system dynamics toward the desirable state E_a, where all agents recycle. This approach aligns with classical deterrence theory, where the combination of high probability and severity of sanctions creates a strong disincentive for non-compliance. However, while increasing p and F may achieve the goal of universal recycling, such measures must be implemented carefully. Excessive penalties or overly frequent enforcement could lead to societal pushback, inefficiencies, or issues of fairness, particularly for agents who may face challenges in meeting recycling requirements. Additionally, the fixed cost of proper recycling may vary significantly across the population or may be difficult to quantify in practical terms. Differences in access to recycling facilities, awareness, or individual effort levels can lead to heterogeneity in k. For these reasons, the case where $k > pF$ may always emerge. In such scenarios, the expected penalties are insufficient to offset the perceived cost of recycling for a significant portion of the population, leading to the persistence of non-recycling behaviors.

For high values of k (that is, $k > pF$), the role of α, which represents the behavioral reward for recycling, becomes particularly significant. When α is sufficiently high, i.e., $\alpha > \max\{v, v/\beta\}$, the system again shifts to Regime 1 (where the only stable fixed point is E_a). This result occurs because the intrinsic and social rewards for recycling outweigh the combined effort costs and fixed costs k. Consequently, all agents are incentivized to recycle, and the system stabilizes at the boundary fixed point E_a. However, recall that for $\beta > 1$, while E_a is still stable, the point E_n, where no agents participate in recycling, can stabilize for $\alpha < v$ (since the point E_1 enters the feasible domain through the border $r = 0$). The point E_n represents a scenario in which the behavioral rewards are insufficient to incentivize recycling, and penalties or enforcement mechanisms fail to overcome the baseline effort cost of recycling. As a result, the population remains entirely disengaged from recycling, leading to the stabilization of E_n. When both boundary points are stable, dynamic Regime 5 is realized, and two basins of attraction are separated by the stable set of the saddle E_1 (the vertical line $r = r_1$), as explained in Sec. 3.

As α decreases past a critical threshold v/β, the stability of E_a is lost, and an interior fixed point, E_2, emerges (due to entering the feasible domain through the border $r = 1$). This fixed point only exists if $\alpha > T$ (with T defined in (14)), reflecting the interplay between the behavioral reward (α) and the effort costs associated with recycling. When $\alpha > T$, the point E_2 becomes the interior attractor for intermediate levels of recycling participation, provided the stability conditions for this point are satisfied. In this regime, r_2, the fraction of agents recycling at E_2, captures a mixed fixed point where both recycling and non-recycling behaviors coexist. Moreover, when $\alpha < v$, the system acquires another attractor at the boundary fixed point E_n implying dynamic Regime 3. In this regime, attained for $T < \alpha < \min[v, v/\beta]$, intriguing dynamics arise when the system exhibits the coexistence of two attractors: (i) either the stable fixed point E_2 or another attractor in its neighborhood $U(E_2)$, representing partial recycling participation, and (ii) E_n, where no recycling occurs. This coexistence reflects a bifurcation in societal behavior, with the final outcome dependent

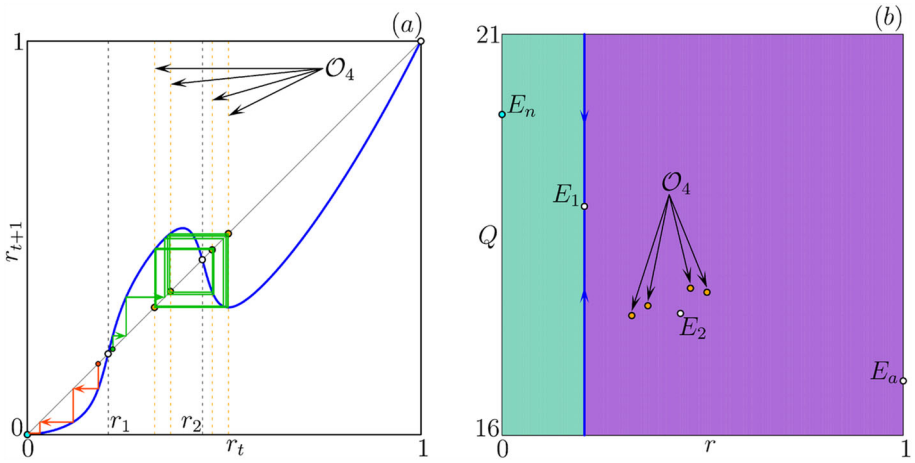

Fig. 3 Coexistence of the stable E_n and a stable 4-cycle $\mathcal{O}_4$ with simply connected basins. Parameter values: $\alpha = 2.3$, $\beta = 0.65$, $\gamma = 0.9$, $k = 19$, $p = 0.8$, $F = 15$, $A = 10$, $K = 1$, $\delta = 0.5$, $\lambda = 6$

on initial conditions. In the following, we will discuss how shifts in population awareness or recycling incentives can tip the system toward either attractor.

We proceed with simulations of the system to analyze the basins of attraction and the dynamics around the fixed point E_2. For this purpose, we specify the function $G(y)$ following the approach in Bischi et al. (2009):

$$G(y) = \frac{2}{\pi} \arctan\left(\frac{\lambda \pi y}{2}\right), \tag{18}$$

where parameter $\lambda > 0$ is the agents' *intensity of choice*. While this specification enables us to explore the behavior of the map and its qualitative properties, it is important to observe that some of the results are tied to this particular form of $G(\cdot)$ in (18) and may not universally apply to all possible functional forms of G. For instance, the variety of asymptotic dynamics in the neighborhood $U(E_2)$, depends on the shape of $\mathcal{S}_1$, which is primarily determined by the function G and its steepness over $\mathbb{R}$. Similarly, the form of G also influences the possibility to have mixed basins, namely, whether the value of a local minimum of $\mathcal{S}_1$ in the interval $(r_2, 1)$ can fall below r_1 (see the remark related to Regime 3 in Sec. 3).

It is known that qualitative transformations of the phase space of a map are closely related to the regions in which points have different number of preimages (more precisely, to boundaries of these regions). Recall that $\mathcal{S}$ is triangular, that is, its first component $\mathcal{S}_1$ is independent of the second variable Q_t. In other words, the dynamics of the first variable can be considered independently of the second variable. Moreover, the second component $\mathcal{S}_2$ is linear with respect to Q_t. It means that the number of preimages of any point is completely defined by the first component $\mathcal{S}_1$.[8] This allows one to effectively describe major qualitative transformations of the phase space by the first row of (11) only. Thus, we can consider the one-dimensional map over r_t defined by the first component $\mathcal{S}_1(r_t)$, to explain how the global dynamics of the two-dimensional map changes.

Example 1. In Figure 3, we illustrate how different initial conditions can lead to different attractors, when Regime 3 with simply connected basins is realized. In the panel (a), map

[8] One can use here the arguments similar to those used in Sec. 3 for explaining transformations of the stable set of the saddle E_1.

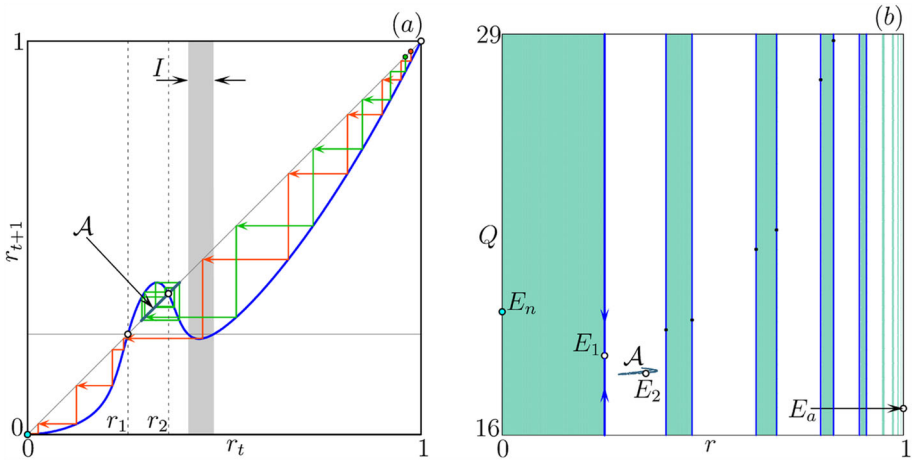

Fig. 4 Coexistence of the stable E_n and a chaotic attractor $\mathcal{A}$ with disconnected basins, each having infinite number of connected elements. Parameter values: $\alpha = 2.3, \beta = 0.613, \gamma = 0.9, k = 19, p = 0.8, F = 15, A = 10, K = 1, \delta = 0.5, \lambda = 10$

$\mathcal{S}_1$ is shown together with the evolution of the first coordinate r. The orbits with initial conditions $r^0 < r_1$ are attracted to E_n (the r-coordinate of a sample orbit is shown orange), while the orbits with $r^0 > r_1$ asymptotically approach a cycle $\mathcal{O}_4$ of period 4, located in the neighborhood $U(E_2)$ of the saddle E_2 (the r-coordinate of a sample orbit is shown green). Dashed gray lines mark r_1 and r_2, while yellow dashed lines mark the r-values of the cycle $\mathcal{O}_4$. In the panel (b), we plot the phase space with the basin of E_n filled light-blue and the one of $\mathcal{O}_4$ shown violet. The two basins are obviously separated by a stable set of the saddle E_1 (blue line with arrows), as described in Sec. 3. Observe that the stable set of the saddle E_a represents the right-hand side boundary (the vertical line $r = 1$) of the feasible state domain.

Example 2. In Figure 4, a more complicated situation is illustrated (Regime 3 with disconnected basins). As one can observe in panel (a), locally in the neighborhood of r_1 the situation is similar to the one in Example 1: the orbits with initial conditions $r^0 < r_1$ approach E_n, while the orbits with $r^0 > r_1$ are attracted to the interior chaotic attractor $\mathcal{A}$ (r-coordinates of its points are marked on the main diagonal by steel-blue dots). However, a local minimum of $\mathcal{S}_1$ goes below the level related to the value r_1 (shown by the horizontal gray line). This implies that some initial conditions located to the right of r_1 produce orbits attracted to E_n. These initial conditions belong to the interval I confined by two appropriate preimages of r_1 (obtained by the inverse $\mathcal{S}_1^{-1}$). Moreover, the interval I has an infinite number of preimages, which accumulate toward $r = 1$ and become smaller and smaller. In such a way, the closer an initial value r^0 to $r = 1$, the more sensitive the dynamics to initial conditions, since the basins of two attractors become highly intermixed. With green and orange, we show r-coordinate of two orbits that end up at two different attractors, although they have initial conditions that are rather close to each other. In panel (b), the phase space is plotted, where the basin of E_n is again shown in light blue, while white color corresponds to orbits asymptotically approaching the chaotic attractor $\mathcal{A}$. The black dots mark several preimages of the saddle E_1 and blue lines show its stable set computed up to a certain point.

The latter findings have significant implications. The presence of multiple intermixed basins of attraction, which alternate infinitely many times, implies that small differences in initial conditions or minor perturbations can lead the system to vastly different long-

term outcomes. This sensitivity underscores the challenges of predicting the population's recycling behavior and the potential difficulty in steering the system toward a desired fixed point. Furthermore, the coexistence of complex attractors, such as periodic cycles, indicates that the dynamics of the system may exhibit temporal oscillations, reflecting fluctuations in recycling behavior over time. From a policy perspective, these results highlight the need for interventions that not only incentivize recycling but also reduce the sensitivity of the system to initial conditions. Strategies that eliminate competing attractors, such as E_n or periodic cycles, could be instrumental in achieving stable and widespread recycling behavior. Understanding the underlying mechanisms that govern these dynamics is essential for designing effective and robust policy measures.

The complexity in the model arises primarily from the dynamics associated with the fixed point E_2, as it is the only fixed point capable of undergoing a flip bifurcation. To examine the conditions that give rise to complex dynamics, we employ two-dimensional bifurcation diagrams using particular sections of the parameter space. We begin with the (k, α) parameter plane shown in Figure 5*a*, where the remaining parameters are fixed as in Figure 4). Clear similarities can be observed when comparing this diagram to the schematic representation in Figure 1*a*. The blue, black, green, and red curves have the same interpretation as in Figures 1, 2, corresponding respectivelly to $k = pF$, $\alpha = T$ (fold bifurcation $\mathcal{F}_{E_1/E_2}$), $\alpha = v$ (transcritical bifurcation of $\mathcal{T}_{E_1/E_n}$), and $\alpha = v/\beta$ (transcritical bifurcation of $\mathcal{T}_{E_2/E_a}$) with T and v defined in (14). The region associated with Regime 1 is shaded light-blue, while the region corresponding to Regime 2 is shaded pink (see the colorbar legend at the bottom of the figure, where these colors are labeled R1 and R2). As explained in Sec. 3, the internal attractor can exist only within the region bounded by the curves $\mathcal{F}_{E_1/E_2}$ and $\mathcal{T}_{E_2/E_a}$, and it coexists with the stable fixed point E_n when $\alpha < v$ (i.e., below $\mathcal{T}_{E_1/E_n}$). Inside this region (between $\mathcal{F}_{E_1/E_2}$ and $\mathcal{T}_{E_2/E_a}$), one observes a rich bifurcation structure characterized by multiple periodicity tongues, whose periods are color-coded according to the horizontal bar at the bottom of the diagram (colors labeled 1 through 20 correspond to respective periods, while white indicates higher periodicity or chaotic attractors). Notably, the shapes of major periodicity regions resemble "shrimps", a well-known feature also observed in other one- and two-dimensional maps, including the classical Hénon map (see, e.g., Kryzhevich et al. (2021) and references therein).

The whole structure is better visible in Figure 5*b*, where the section (β, λ) of the parameter space is plotted for $\alpha = 2.3$, $k = 19$, and $F = 16.3$.[9] Since the chosen value of F implies $\alpha < v$, for the whole range of β and λ, the fixed point E_n is stable. Hence, for $\beta < 2\sqrt{v/\alpha - 1}$ (with the latter value corresponding to $\mathcal{F}_{E_1/E_2}$), Regime 2 is attained, for $2\sqrt{v/\alpha - 1} < \beta < v/\alpha$ (with the second threshold associated with $\mathcal{T}_{E_2/E_a}$), the internal attractor coexists with E_n (Regime 3), and for $\beta > v/\alpha$, two stable boundary fixed points lead to Regime 5 (the corresponding region is colored lilac, labeled in the colorbar as R5). A particular feature of the bifurcation structure related to nontrivial dynamics, which catches one's eye, is that at both sides of the "central" region related to period two, there are two sequences of regions associated with the same sequences of periods, organized according to the order that is somewhat similar to the period adding.[10] Though the source and the relevancy of such an analogy require deeper investigation.

[9] Note that the value of $F = 16.3$ is chosen to be close to but less than the threshold $(k\gamma - \alpha^2)/(p\gamma)$, which corresponds to $\mathcal{T}_{E_1/E_n}$, so that the region related to nontrivial dynamics is wider and the related structure is better visible.

[10] Indeed, between regions associated with periods 2 and 3 there is a region related to period 5, between periods 2 and 5 there is period 7, between 3 and 5 there is period 8, between 3 and 4 there is period 7, etc.

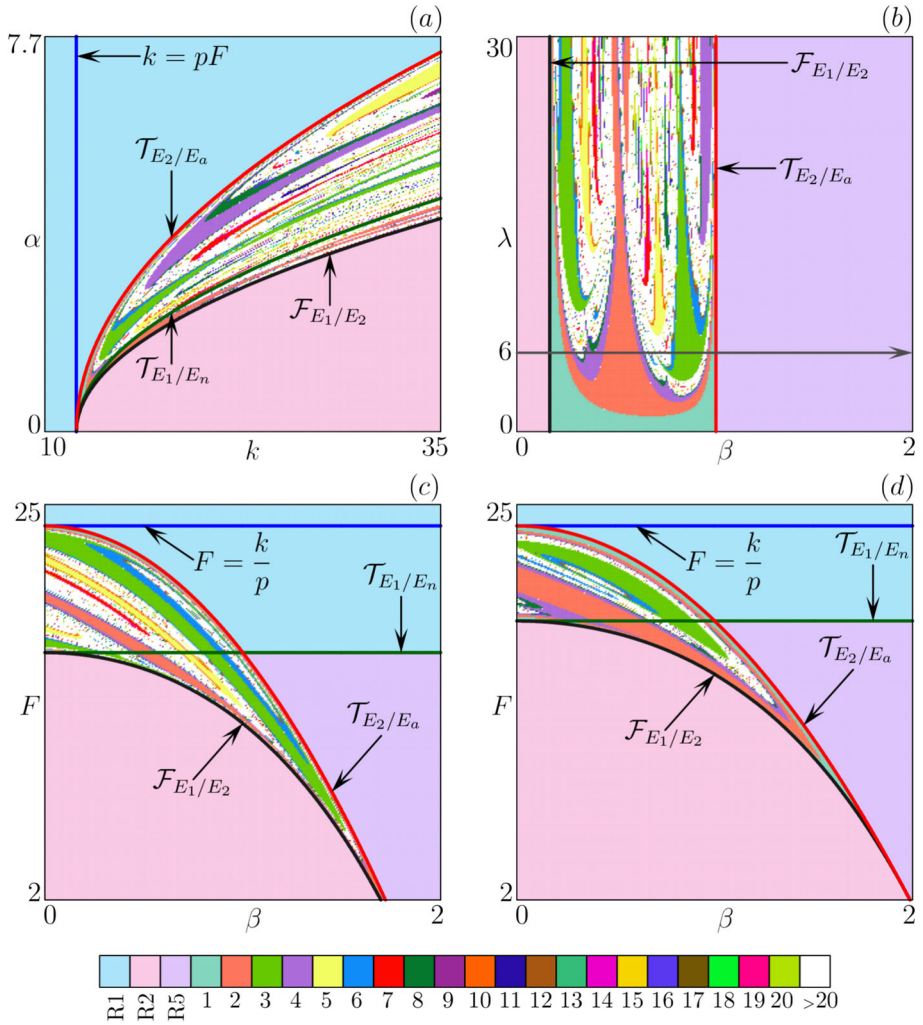

Fig. 5 2D bifurcation diagrams for map $\mathcal{S}$ in (a) (k, α); (b) (β, λ); (c, d) (β, F) parameter planes. Colors labeled 1 through 20 correspond to cycles of respective periods, white color means higher periodicity or chaos. Colors labeled R1, R2, and R5 are associated with Regimes 1, 2, and 5. The blue line is defined by $k = pF$. The black line marks the fold bifurcation of E_1 and E_2. The green and the red lines correspond to the transcritical bifurcations of E_1/E_n and E_2/E_a, respectively. In (a) $\beta = 0.613$, $F = 15$, $\gamma = 0.9$, $\lambda = 10$; in (b)–(d) $\alpha = 2.3$, $k = 19$ with $F = 15$, $\gamma = 0.9$ (b), $\lambda = 10$, $\gamma = 0.9$ (c), and $\lambda = 6$, $\gamma = 1.2$ (d). The other parameters are $p = 0.8$, $A = 10$, $K = 1$, $\delta = 0.5$

As the current paper is mostly aimed at focusing on applied aspects, we do not provide any detailed description of the bifurcation structure observed, leaving this task for the future. We only remark that it is most likely caused by the bimodal shape of the first component $\mathcal{S}_1$ (cf. Figures 3*a*, 4*a*) and can be effectively described by considering a one-dimensional map of the respective form. An additional argument supporting this hypothesis is that the bifurcation structure is especially sensitive to changing λ. In Figure 5*b*, it can be noticed that the increase of λ leads to the appearance of more periodicity regions corresponding to stable

cycles of different periods. Indeed, λ regulates the steepness of G, indirectly influencing the shape of $\mathcal{S}_1$ (the value of local minimum and maximum and the overall steepness of $\mathcal{S}_1$ in the neighborhood of E_2). In other words, increasing λ increases complexity (which is not surprising, taking into account that λ represents agents' speed of reaction to utility differences). This can be further observed in the panels c and d of Figure 5, where (β, F) parameter plane is plotted for $\lambda = 10$ and $\lambda = 6$, respectively. With smaller λ the bifurcation structure, related to the internal attractor, becomes obviously simpler. Two last panels also differ by the value of γ, which is $\gamma = 0.9$ in c and $\gamma = 1.2$ in d. Changing γ obviously reshapes the boundaries of the region related to complex dynamics. With larger γ (panel d), the threshold related to the transcritical bifurcation $\mathcal{T}_{E_1/E_n}$ shifts to higher value of F, while the region with complex dynamics becomes thinner and its lower part drifts to the right. This entails enlargement of the region associated with Regime 2 (where no agents participate in recycling), indicating that, to drive the system to the desired Regime 1 (where the entire population adopts recycling behavior), with increasing γ, stricter penalties are required (larger F), as well as a higher willingness of agents to participate in common activities (larger β).

In Figure 6 we plot the evolution of the first coordinate r with respect to the parameter β for $\lambda = 6$ (the related path is marked by the gray arrow in Figure 5*b*). As has been mentioned above, for the whole range of β the fixed point E_n is stable and it is marked by the cyan line. The dashed green curve shows r_1, while the dashed orange curve marks the local minimum value $\min_{r\in(r_2,1)} S_1(r)$, when it exists (namely, when the eigenvalue λ_1 of E_2 is negative). Obviously, this minimum value never falls below r_1. Thus, the basins of two coexisting attractors are simply connected, and for $\beta > 2\sqrt{v/\alpha - 1}$ (after the fold bifurcation $\mathcal{F}_{E_1/E_2}$, marked by the black vertical line), the basin of E_n becomes rather small.

From the applied perspective, Figure 6 reveals how changes in β influence the system's behavior, illustrating a transition from order to chaos: for high values of β, the system exhibits stable and predictable dynamics, for the major part of initial conditions with $r^0 > r_1$. In this regime, the recycling behavior of the population settles into a steady state with a high share of conscious agents r (either E_2 or E_a). This reflects a societal context where agents derive their utility from collective participation, and strong alignment between social norms and behavioral incentives promotes stability. However, as β decreases, the system begins to exhibit successive bifurcations, marking the onset of chaotic dynamics. These bifurcations reflect a breakdown of stability, with E_2 losing its attractor properties and giving rise to increasingly complex behaviors. The transition to chaos is marked by regions of periodicity interspersed within the chaotic regime, where the system temporarily settles into periodic cycles before returning to a chaotic state. Socially, this corresponds to a scenario where agents' motivations become more individualistic (decreasing β), reducing the reinforcing effect of collective participation. As a result, small fluctuations in behavior amplify over time, leading to unpredictability and disorder in the population's recycling dynamics. For regulators, these findings suggest that awareness policies that increase the value of β could be an effective strategy to prevent chaotic behaviors. By fostering stronger social norms and reinforcing collective motivations, policymakers could create an environment where agents perceive greater utility from aligning with widespread participation in recycling. Such interventions could stabilize the system and ensure predictable outcomes, reducing the risks associated with chaotic dynamics.

Figure 7 differs from Figure 6 only by the enlarged value $\gamma = 1.2$, while the other parameters remain unchanged. The meaning of the solid lines and the dashed curves is the same as before. Again for $\beta > 2\sqrt{v/\alpha - 1}$, the basins of two coexisting attractors are simply connected (since $\min_{r\in(r_2,1)} S_1(r) > r_1$). However, the basin of E_n is now larger (as indicated by the value r_1), which supports conclusions made above when comparing the panels c and

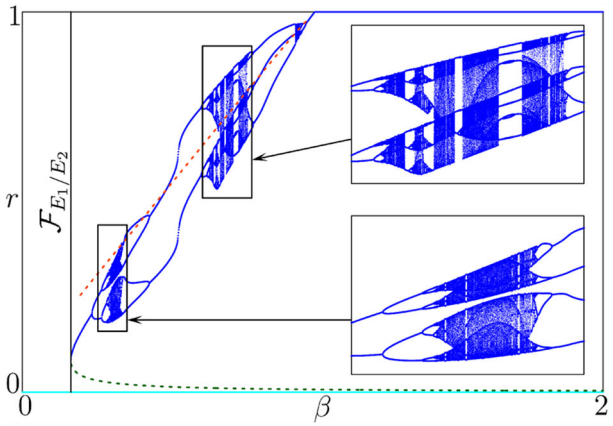

Fig. 6 Evolution of the first coordinate r w.r.t. β for $\lambda = 6$ and the other parameters as in Figure 5*c* (where the respective path is marked by the gray arrow)

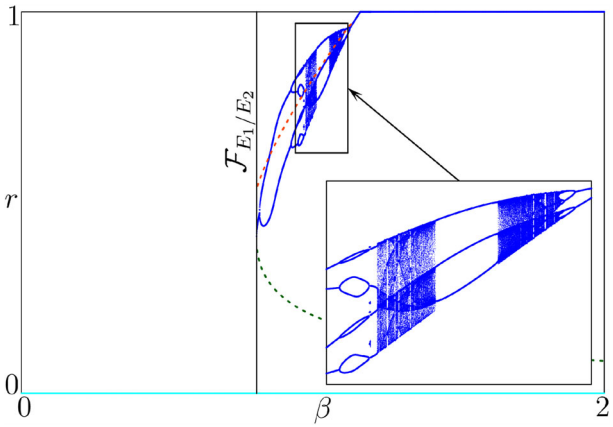

Fig. 7 Evolution of the first coordinate r w.r.t. β for the same parameter set as in Figure 6, except for $\gamma = 1.2$

d of Figure 5, i.e., when recycling effort becomes more costly (γ increases), regulators should adopt tougher punishment and use methods that favour increasing agents' social consciousness. We would also like to draw the reader's attention to another phenomenon, revealed in Figure 7 in contrast to Figure 6. For a narrow range of intermediate values of β, there is a coexistence of two internal attractors (this phenomenon is better visible in the inset, where the related part of the bifurcation diagram is enlarged). Identifying conditions for such coexistence is possible and requires thorough studies. We postpone this analysis for future work.

Comparing Figures 6 and 7 from the applied viewpoint, we observe that if γ is smaller, more virtuous behavior can be obtained for a greater range of values of β. This suggests that legislation that can reduce γ, i.e., make the recycling process less labor-intensive, can support a greater presence of conscious agents for a wider range of possible social norms (i.e., for a greater range of β).

Lastly, we turn our attention to the dynamics of the system in two distinct societal configurations characterized by the parameter β, which reflects the societal perception of recycling

rewards based on collective participation. In societies where $\beta = 0$, agents derive maximum utility from recycling when few individuals participate, emphasizing a sense of moral distinction or exclusivity. Under these conditions, the system exhibits distinct behaviors depending on the value of α. The findings and discussions presented thus far can be summarized as follows, offering key insights for policymakers aiming to promote sustainable recycling behavior:

- One of the most effective interventions is to ensure that the perceived baseline effort cost of recycling is lower than the expected penalties for non-compliance. This approach can theoretically push the population toward universal recycling. However, implementing such a strategy is challenging. Excessively high penalties or control probabilities may lead to resistance, fairness concerns, or other unintended consequences. Moreover, for some individuals or groups, the perceived effort cost may remain high due to structural or psychological barriers, limiting the effectiveness of this approach.
- A more practical and broadly applicable intervention is to increase the intrinsic and social rewards associated with recycling. Raising these rewards can directly offset the perceived effort cost and drive higher participation rates. Effective policies in this regard include public campaigns to raise awareness, programs that socially reward recycling efforts, and targeted incentives that align individual actions with collective goals.
- When behavioral rewards are at intermediate levels, the system may exhibit a multiplicity of attractors, including complex or chaotic dynamics. Such outcomes can lead to unpredictable recycling behavior, where different behavioral patterns coexist. To prevent these scenarios and encourage stable recycling dynamics, policymakers should prioritize strategies that enhance societal coherence. Specifically, increasing the perception of collective participation as a valued norm reduces the risk of instability and promotes widespread adoption of recycling.
- Among the societal configurations analyzed, those that strongly value collective participation are the most capable of achieving high levels of recycling. Societies where individuals derive utility from widespread participation are naturally aligned with universal recycling outcomes. However, these outcomes depend on maintaining sufficiently high behavioral rewards and ensuring that the population is sensitive and responsive to changes in perceived utility. Policymakers should foster environments where individuals are both motivated and capable of adapting their behavior to align with societal norms.

5 Conclusion

We have analyzed two types of agents with distinct responses to recycling incentives: unconscious and conscious agents. Unconscious agents are disengaged from recycling, deriving no intrinsic or social rewards from it, and remain unaffected by institutional or behavioral interventions, making them difficult to influence through traditional policies.

Conscious agents, in contrast, actively recycle, balancing effort costs with rewards from intrinsic motivations and societal dynamics. Their utility depends on both their effort and the level of participation in the population, increasing with broader collective involvement but diminishing when recycling becomes overly common. This makes them responsive to interventions that enhance social norms and collective action. We also examine societal scenarios where recycling is most rewarding as either a rare individual effort or a widely shared communal practice, reflecting diverse cultural values.

We found that effective interventions to promote recycling behavior rely on balancing individual costs, enforcement mechanisms, and societal motivations. Ensuring that the perceived effort cost of recycling is lower than the expected penalties for non-compliance can theoretically drive universal recycling. However, this approach is challenging, as excessive penalties or enforcement may provoke resistance and fairness concerns, and structural barriers can make recycling seem costly for some individuals. A more practical strategy is to enhance the intrinsic and social rewards of recycling, offsetting perceived effort costs and encouraging participation. Public awareness campaigns, social recognition programs, and targeted incentives are effective tools to align individual actions with collective goals. When behavioral rewards are moderate, the system may exhibit multiple attractors, including complex or chaotic dynamics. To avoid these scenarios and ensure stable recycling, policymakers should enhance societal coherence by promoting collective participation as a valued norm. This reduces instability and fosters widespread adoption of recycling. Finally, societies that value collective participation are best positioned to achieve high recycling rates, provided behavioral rewards are sufficiently strong and the population is responsive to utility changes. Policies should focus on fostering environments where individuals are motivated and able to align their behavior with collective norms, ensuring sustainable and cohesive recycling practices.

A APPENDIX

A.1 Evolutionary dynamics through Word-of-Mouth

The probability of switching behavior from unconscious to conscious, given that $\pi_c \geq \pi_u$, is

$$\Phi(y) = \mathbb{P}(u \to c | \pi_c \geq \pi_u),$$

where Φ is the non-decreasing probability distribution function, $y = \pi_c - \pi_u$, $\lim_{y \to -\infty} \Phi = 0$ and $\lim_{y \to +\infty} \Phi = 1$. It follows that the probability of an unconscious agent becoming conscious is

$$p_{u \to c} = r\Phi(y)$$

and consequently it has $p_{u \to u} = 1 - r\Phi(y)$, while the probability of a conscious agent becoming unconscious is

$$p_{c \to u} = (1 - r)[1 - \Phi(y)]$$

from which it follows $p_{c \to c} = 1 - p_{c \to u}$.

We assume that the matching between agents within the population is uniformly random and that a sufficiently large sample of pairings is drawn. Under these conditions, the average utility difference between the two behaviors can be approximated by the expected utility difference:

$$y(r) = \mathbb{E}[\pi_c] - \mathbb{E}[\pi_u].$$

The fraction r_t of conscious agents at time evolves based on the interactions between conscious and unconscious agents. Each interaction influences behavior according to the relative utilities of the two types of agents. The change in r_t over time captures the dynamics of social learning and adaptation. The dynamics are governed by

$$r_{t+1} = r_t + (1 - r_t)\, p_{u \to c} - r_t\, p_{c \to u},$$

where $(1 - r_t)p_{u\to c}$ is the share of unconscious agents becoming conscious and $r_t\, p_{c\to u}$ is the share of conscious agents becoming unconscious, based on the utility difference. After a few straightforward algebraic steps, the previous function can be written as

$$r_{t+1} = r_t\big[1 + (1 - r_t)G\big(y(r_t)\big)\big], \tag{19}$$

where $G(y(r_t)) = 2\Phi(y(r_t)) - 1$. Function G captures the net effect of individuals switching behaviors—either from being unconscious to conscious or vice versa—based on the utility differential $y(r_t)$. Moreover, it has several key properties that make it suitable for modeling these dynamics. First, it is strictly increasing, meaning the larger the utility differential, the greater the absolute value of G. This reflects the intuitive idea that stronger utility advantages lead to more pronounced behavioral shifts. Second, it is bounded between -1 and 1, ensuring realistic limits on the rate of change in the population. A value of $G = 1$ implies maximum growth in the conscious population, while $G = -1$ represents the fastest possible decline. The function is symmetric and ensures that $G(0) = 0$, meaning no net change occurs when the utilities are equal. Additionally, function G is odd, reflecting the symmetry of the system: if the roles of conscious and unconscious agents are reversed, the dynamic change in r_t simply mirrors the original, ensuring that the model remains balanced. It is also differentiable at $y = 0$, ensuring smooth transitions when the utility difference is negligible. Lastly, G is convex for negative values of y and concave for positive values, capturing how the rate of change accelerates or decelerates depending on the utility differential. This convex-concave structure highlights that small utility advantages produce modest behavioral shifts, while large utility differences drive greater changes. Mathematically, the assumptions and properties on G can be summarized as follows:

- $G(0) = 0$;
- $-1 \le G(y) \le 1$;
- $G(-y) = -G(y)$;
- $G \in \mathcal{C}^2$;
- $G'(y) > 0, \quad \forall y \in \mathbb{R}$;
- $G''(y) \ge 0 \quad \text{for } y \in \mathbb{R}_-,\ G''(y) \le 0 \quad \text{for } \in \mathbb{R}_+$.

Clearly, $G(y)$ serves as a cornerstone for understanding the evolution of conscious agents within the population and sets the foundation for the analysis of long-term fixed points and dynamic stability.

Acknowledgements The work Anastasiia Panchuk is funded by the PRIN 2022 under the Italian Ministry of University and Research (MUR) Prot. 2022YMLS4T – TEC – Tax Evasion and Corruption: theoretical models and empirical studies. A quantitative-based approach for the Italian case.

Funding Open access funding provided by Università degli Studi di Urbino Carlo Bo within the CRUI-CARE Agreement.

Declarations

Competing interests Francesca Grassetti and Fabio Lamantia declare having provided consultancy within the "PRIN PNRR 2022 P20227XP7P - SWAMSI: Solid WAste Management in South Italy" project, funded under the PRIN-PNRR program, which contributed to the results presented in this article.

References

Atri, S., & Schellberg, T. (1995). Efficient management of household solid waste: a general equilibrium model. *Public Finance Review, 23*(1), 3–39. https://doi.org/10.1177/109114219502300101

Barr, S., Gilg, A. W., & Ford, N. J. (2001). A conceptual framework for understanding and analysing attitudes towards household-waste management. *Environment and Planning A, 33*(11), 2025–2048. https://doi.org/10.1068/a33225

Bortoleto, A. P., Kurisu, K. H., & Hanaki, K. (2012). Model development for household waste prevention behaviour. *Waste Management, 32*(12), 2195–2207. https://doi.org/10.1016/j.wasman.2012.05.037

Bischi, G. I., Lamantia, F., & Sbragia, L. (2009). Strategic interaction and imitation dynamics in patch differentiated exploitation of fisheries. *Ecological Complexity, 6*(3), 353–362. https://doi.org/10.1016/j.ecocom.2009.03.004

Corsini, F., Gusmerotti, N.M., Testa, F., Iraldo, F. Exploring waste prevention behaviour through empirical research. Waste Management 79, 132–141 (2018) https://doi.org/10.1016/j.wasman.2018.07.037.

Dawid, H. (1999). On the dynamics of word of mouth learning with and without anticipations. *Annals of Operations Research, 89*, 273–295.

Di Vita, G. (2001). Technological change, growth and waste recycling. *Energy Economics, 23*(5), 549–567. https://doi.org/10.1016/S0140-9883(01)00075-5

Eichner, T., & Pethig, R. (2001). Product design and efficient management of recycling and waste treatment. *Journal of Environmental Economics and Management, 41*(1), 109–134. https://doi.org/10.1006/jeem.2000.1130

Eichner, T., & Pethig, R. (2003). Corrective taxation for curbing pollution and promoting green product design and recycling. *Environmental & Resource Economics, 25*(4), 477–500. https://doi.org/10.1023/A:1025057712785

Fiorino, D. J. (2020). Personal behavior, motivation, and the pursuit of sustainability. *Environmental Economics and Policy Studies, 22*(4), 553–570. https://doi.org/10.1007/s10018-020-00270-2

Goh, E., Esfandiar, K., Jie, F., Brown, K., Djajadikerta, H. Please sort out your rubbish! an integrated structural model approach to examine antecedents of residential households' waste separation behaviour. Journal of Cleaner Production 355, 131789 (2022) 10.1016/j.jclepro.2022.131789.

Highfill, J., & McAsey, M. (1997). Municipal waste management: Recycling and landfill space constraints. *Journal of Urban Economics, 41*(1), 118–136. https://doi.org/10.1006/juec.1996.1096

Hamilton, S., Sproul, T. W., Sunding, D., & Zilberman, D. (2013). Environmental policy with collective waste disposal. *Journal of Environmental Economics and Management, 66*(2), 337–346. https://doi.org/10.1016/j.jeem.2013.04.003

Huhtala, A. (1997). A post-consumer waste management model for determining optimal levels of recycling and landfilling. *Environmental & Resource Economics, 10*(3), 301–314. https://doi.org/10.1023/A:1026475208718

Kryzhevich, S., Avrutin, V., Söderbacka, G. Bistability in a one-dimensional model of a two-predators-one-prey population dynamics system. Lobachevskii Journal of Mathematics 42, 3486–3496 (2021) https://doi.org/10.1134/S1995080222020135.

Kipperberg, G., & Larson, D. (2012). Heterogeneous preferences for community recycling programs. *Environmental & Resource Economics, 53*(4), 577–604. https://doi.org/10.1007/s10640-012-9578-y

Klöckner, C.A., Oppedal, I.O. General vs. domain specific recycling behaviour-applying a multilevel comprehensive action determination model to recycling in norwegian student homes. Resources, Conservation and Recycling 55(4), 463–471 (2011) https://doi.org/10.1016/j.resconrec.2010.12.009.

Lamantia, F., Pezzino, M. Social norms and evolutionary tax compliance. The Manchester School 89, 385–405 (2021) https://doi.org/10.1111/manc.12368.

Lafforgue, G., Rouge, L. A dynamic model of recycling with endogenous technological breakthrough. Resource and Energy Economics 57, 101–118 (2019) https://doi.org/10.1016/j.reseneeco.2019.04.002.

Mazzanti, M., & Zoboli, R. (2008). Waste generation, waste disposal and policy effectiveness: Evidence on decoupling from the european union. *Resources, Conservation and Recycling, 52*(10), 1221–1234. https://doi.org/10.1016/j.resconrec.2008.07.003

Nishimura, K. (2002). On inefficiency and instability in decentralized recycling systems. *Environmental Economics and Policy Studies, 4*(3), 210. https://doi.org/10.1007/BF03354015

Pakpour, A. H., Zeidi, I. M., Emamjomeh, M. M., Asefzadeh, S., & Pearson, H. (2014). Household waste behaviours among a community sample in iran: An application of the theory of planned behaviour. *Waste Management, 34*(6), 980–986. https://doi.org/10.1016/j.wasman.2013.10.028

Reijonen, H., Bellman, S., Murphy, J., Kokkonen, H. Factors related to recycling plastic packaging in finland's new waste management scheme. Waste Management 131, 88–97 (2021) https://doi.org/10.1016/j.wasman.2021.05.034.

Smith, V. L. (1972). Dynamics of waste accumulation: Disposal versus recycling. *The Quarterly Journal of Economics, 86*(4), 600–616.

Shi, J.-G., Xu, K., Si, H., Song, L., Duan, K. Investigating intention and behaviour towards sorting household waste in chinese rural and urban–rural integration areas. Journal of Cleaner Production 298, 126827 (2021) 10.1016/j.jclepro.2021.126827.

Thomas, C., Sharp, V. Understanding the normalisation of recycling behaviour and its implications for other pro-environmental behaviours: A review of social norms and recycling. Resources, Conservation and Recycling 79 (2013) https://doi.org/10.1016/j.resconrec.2013.04.010.

Valente, M. (2023). Policy evaluation of waste pricing programs using heterogeneous causal effect estimation. *Journal of Environmental Economics and Management, 117*, Article 102755. https://doi.org/10.1016/j.jeem.2022.102755

Xu, L., Ling, M., Lu, Y., & Shen, M. (2017). Understanding household waste separation behaviour: Testing the roles of moral, past experience, and perceived policy effectiveness within the theory of planned behaviour. *Sustainability, 9*(4), 625. https://doi.org/10.3390/su9040625

Yan, L., & Murray, K. B. (2023). The motivational dynamics of arousal and values in promoting sustainable behavior: A cognitive energetics perspective. *International Journal of Research in Marketing, 40*(3), 679–699. https://doi.org/10.1016/j.ijresmar.2022.12.004